

High resolution displacement monitoring of a slow velocity landslide using ground based radar interferometry

B. Lowry^{a,*}, F. Gomez^b, W. Zhou^a, M.A. Mooney^a, B. Held^b, J. Grasmick^a

^a Colorado School of Mines, Golden, CO, United States

^b University of Missouri at Columbia, Columbia, MO, United States

ARTICLE INFO

Article history:

Received 18 October 2012

Received in revised form 8 July 2013

Accepted 14 July 2013

Available online 19 July 2013

Keywords:

Landslides

Remote Sensing

Radar

Interferometry

Monitoring

Terrestrial geodesy

ABSTRACT

Ground-based interferometric radar (GBIR) monitoring was conducted on a slow-moving, translational failure landslide in Granby, Grand County, Colorado, USA. Radar monitoring was completed over two separate surveys in 2011 using a tripod mounted real aperture sensor. The purpose of this work is to evaluate GBIR as a temporally dense monitoring technique for monitoring landslide displacement and compare the monitoring results to ongoing GPS based surveying methods to verify measured displacements. We discuss the strengths and limitations of GBIR displacement monitoring with a variety of available sensors, and place this monitoring platform, sensor, and workflow into context of previous slope stability monitoring with GBIR. For both surveys, displacement time series were created through a small temporal baseline stacking to reduce noise and maintain high temporal resolution. The results of the displacement time series were compared to average displacement rates derived from GPS based surveying. An overall verification of radar and GPS derived displacement rates was achieved, and identifies important differences relating to the precision and uncertainty of the two techniques. This work demonstrates GBIR monitoring capability of establishing high temporal resolution on tracking variable rates of landslide movements. Spatial modeling of total observed displacements was completed for both surveys verifying a conceptual model of uniform translational landslide movement, providing greater confidence for mitigation planning.

© 2013 Published by Elsevier B.V.

1. Introduction

The use of ground-based interferometric radar (GBIR) sensors has become increasingly valuable to the monitoring of displacements of landslides and unstable slopes. These sensors join a geodetic toolset used to monitor landslides alongside laser-based Light Detection and Ranging (LiDAR), global positioning systems (GPS), and photogrammetric imaging. GBIR monitoring enables imaging of ground surface deformation across large areas (<10 km²) with high spatial (<1 mm) and temporal (<1 h. scan frequency) resolutions. GBIR systems have been successfully implemented for landslide monitoring with good examples presented in literature across a range of sensor types (Leva et al., 2003; Tarchi et al., 2003; Noferini et al., 2007; Barla et al., 2010; Casagli et al., 2010; Schulz et al., 2012). Table 1 summarizes these works by slope failure type, spatial and temporal resolution, sensor type, and analytical method. The use of GBIR monitoring has been accelerated by the adaptation of satellite-based interferometry software and analysis techniques. Using these advanced algorithms, and with more control over the platform scanning position, GBIR monitoring has distinct advantages for landslide monitoring applications. However, GBIR

monitoring must be conducted with knowledge of limitations and integrated with traditional displacement monitoring to become a reliable and trusted landslide monitoring tool.

This paper presents a high resolution displacement monitoring application of a slow moving (according to Cruden and Varnes, 1996) landslide using GBIR verified with GPS surveying techniques. The landslide is located near Granby, Grand County, Colorado, USA (Granby landslide hereafter). Radar monitoring was conducted with a Gamma Portable Radar Interferometer (GPRI), a tripod-mounted, rotational scanning radar system with three-antenna real aperture imaging (Figure 1). This sensor uses one antenna to transmit and two receiver antennas, which can be configured for polarimetry or from multiple baselines to subtract topographic effects. The GPRI sensor is formally described in Werner et al. (2008) which addresses issues of instrument sensitivity and specific hardware configuration. This sensor differs from other platforms used to monitor landslides in its use of a real (as opposed to synthetic) aperture, a tripod mount, and rotational scanning action (as opposed to track-based), creating a platform-specific set of considerations for conducting displacement measurement monitoring.

Two sets of scans were carried out in the summer of 2011; in June for a 24-hour span and in August for a 36-hour span. Scans were carried out non-disruptively and independently from existing construction activities such as vehicle movement on the landslide, meaning that some imagery would not be useable for generating landslide displacements.

* Corresponding author. Tel.: +1 720 771 2753.
E-mail address: blowry@mines.edu (B. Lowry).

Table 1
Examples of GBIR monitoring of landslides by sensor and analysis method.

Study	Location	Failure type	Range resolution	Azimuth resolution at 1000 m	Temporal resolution (approx.)	Sensor	Analysis method
Leva et al. (2003)	Schwaz, Austria	Debris flow	2 m	4 m	30 min	Linear SAR-LISA	Interferogram stacking
Tarchi et al. (2003)	NE Italy	Tessina landslide roto-translational	2 m	4 m	50 min	Linear SAR-LISA	Interferogram stacking
Noferini et al. (2007)	NE Italy	Rotational rock block slide	5 m	15 m	30 min	GB-InSAR	Permanent scatterers
Barla et al. (2010)	NW Italy	Deep seated gravitational slope deformation (DSGD)	0.5 m	4.5 m	20 min	GB-InSAR	Permanent scatterers
Casagli et al. (2010)	Italy	Reunion landslide, Stromboli volcano	2 m	2 m	10 min	Linear SAR-LISA	Spatial averaging
Schulz et al. (2012)	Lake City, Colorado, USA	Slumgullion landslide complex	0.75 m	4.375 m	10 min	IBIS-L GB-InSAR	Permanent scatterers
This work	Granby, Colorado, USA	Translational landslide	0.75 m	7 m	7.5 min–15 min	Gamma GPRI real aperture	Interferogram stacking using temporal baseline

Radar interferometry measurement of displacement is necessarily conducted within the sensor line of sight (LOS), requiring geometric adjustment into a corrected displacement model for use in characterizing landslide kinematics, facilitated in this application by survey data. Specifically, this paper presents a case study of a particular sensor combination of GBIR and GPS monitoring on an active slow moving landslide. Generally, this work adds to the large range of application types and sensors as well as addresses how methods of analysis contribute to greater understanding of the use of GBIR in unstable slope and landslide monitoring. GBIR imaging provides a continuous field of displacement measurement serving to fill in the gaps between survey monuments, but measurements are subject to issues with image quality, line of sight correction, phase aliasing, and the specific configuration of the GBIR sensor used to acquire the imagery. This paper addresses these issues specific to a landslide monitoring context using a newly available sensor and presents a comparison with GPS surveying to verify the sensor displacement measurements and suitability of the platform for landslide monitoring. We discuss analytical approaches to optimizing the use of the imaging and processing tools to image the landslide, as well as the implications of the large increase in data collection capacity and temporal granularity provided by this remote sensing platform.

1.1. Landslide monitoring radar interferometry from terrestrial platforms

The technique of radar interferometry relies on comparison of the phase differences between the backscatter of repeated radar scans. This technique allows for measurement of millimeter scale displacement with radio wavelengths within the radar band (approx. 1 mm–30 cm), making the technique particularly suitable for tracking active

landslides over a range of velocities. While success in landslide monitoring using spaceborne differential interferometric synthetic aperture radar (D-InSAR) has been demonstrated (Hilley et al., 2004; Strozzi et al., 2005), satellite-based monitoring in general suffers fundamental challenges with non-zero baselines and sensor LOS obliquity to down-slope landslide movements (Cascini et al., 2010). The fixed orbital periodicities of satellite platforms range from days to weeks, preventing fine temporal scale (<1 h) monitoring of dynamically moving landslides. Other challenges in spaceborne investigations arise from variable spatial baselines between satellite positions, unresolvable phase ambiguities, and temporal decorrelation of signal in the target terrain (Colesanti and Wasowski, 2006).

In ground based platforms, the radar scanning location can be positioned to reduce effects resulting from the obliquity between the radar's LOS and landslide displacement direction. Imagery acquired from the same platform location effectively becomes a zero spatial baseline set of radar images, simplifying the workflow to monitor temporal changes from scan to scan. Small scan intervals (<1 h) and a zero spatial baseline across scans allow for significantly improved control over interferogram quality by reducing temporal decorrelation, and providing real time data acquisition.

Joint GBIR and GPS based monitoring enable the measurement of fascinating behaviors: Schulz et al. (2009) presented GPS and geotechnical monitoring data that revealed displacement rate sensitivity to atmospheric tides within the Slumgullion landslide. Follow-up monitoring with a ground based synthetic aperture radar (GB-InSAR) in Schulz et al. (2012) further verified displacement measurements by correlating kinematic elements a variety of displacement datasets collected over decades of investigation. The Slumgullion project is a good example of how high resolution techniques can be used to characterize a spatially variable landslide with many sources of corresponding displacement monitoring methods on long time scales. Further integration of GBIR imaging workflows with GPS displacement monitoring is important to more understanding of spatial and temporal landslide dynamics as well as provides models for integrating GBIR into typical geotechnical investigations.

2. Granby landslide overview

2.1. Existing displacement monitoring challenges

Information about the Granby landslide has been gathered in an effort to assess stabilization options under a Request for Proposal document issued by Grand County in late 2011, which presents preliminary geotechnical investigation details (Grand County Government and Gagnon, 2011). The Granby landslide has a surface area of approximately 160,000 m² (40 acres) and is moving in a southwesterly direction. Traditional GPS based surveying performed at this landslide was collected independently by engineering consultants and is conducted on bi-weekly or monthly schedules, limiting the temporal resolution to the average velocity occurring between these visits. These visits require a



Fig. 1. Deployed GPRI system and field of view of landslide.

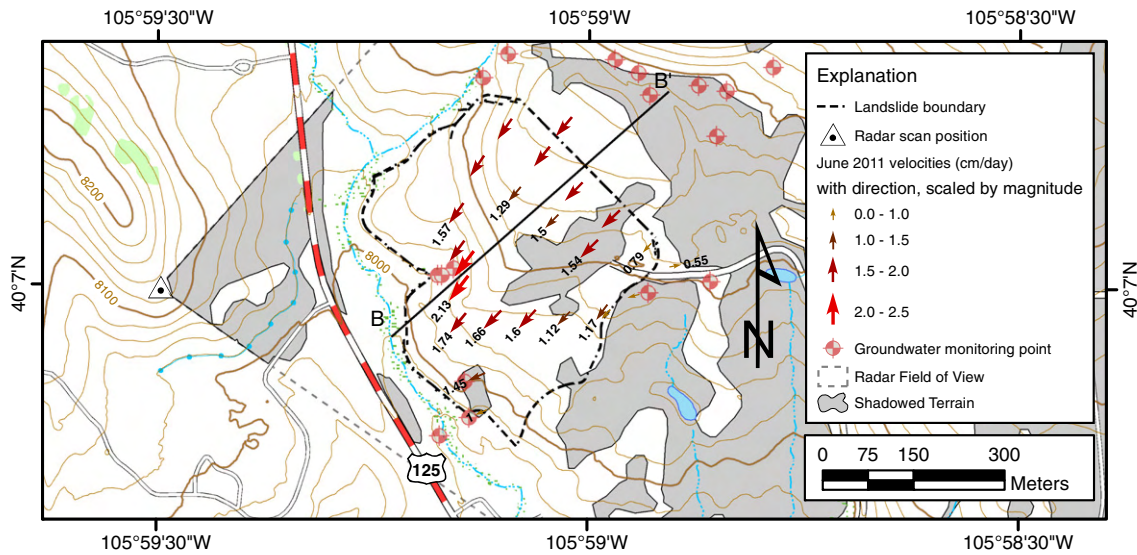


Fig. 2. Layout of radar scan location and independently mapped landslide block extent with geotechnical instrumentation including groundwater monitoring points, survey monuments with GPS velocities during June 2011.

full day of the surveyor's time to collect all the points of interest in the project area. Without significant additional instrumentation, this GPS based surveying prevents efficient measurement of daily movement of the landslide and can only resolve displacements that exceed the sensitivity of the GPS device. Furthermore, GPS surveying methods only tracks a limited number of points on the landslide mass that are vulnerable to destruction during mitigation activities and landslide movement. The resulting point-based dataset requires interpolation of displacement values across measurements. Subsurface monitoring can be conducted from boreholes, but this monitoring is necessarily limited to short term monitoring due to casing shearing from landslide movements. The RTK measurements represent averages of 3 GPS measurements taken over 180 second epochs which was deemed to be repeatable and reliable for this survey site. However, GPS accuracy is dependent on a host of different factors including atmospheric delay, systematic errors, post processing and accuracy is commonly accepted at 1–5 cm under ideal conditions (Rizos, 1999; Bossler et al., 2002; Lee and Ge, 2006).

The spatial extent and direction of the landslide movement is illustrated by the vector plot shown in Fig. 2. The vectors represent displacement during the month of June, 2011 derived from the GPS-based survey. The subsurface investigation revealed a translational slip plane at a maximum depth of approximately 27 m illustrated in an interpreted cross section in Fig. 3. Evidence of multiple remnant slip planes was found in the boring logs, consistent with landslide footprint being located in a mapped landslide deposit (Schroder, 1995). The slip planes consist of weak clay layers that lie within the Middle Park Formation of Eocene–Paleocene (depicted in gray in Figure 3), a unit of Tertiary Period composed of sandstone and shale. The sliding mass is made up of intermingled Middlepark, colluvium, and the reactivated sliding surface has progressed into the landfill material. Monitoring of boreholes indicated an active slip plane both through removable inclinometers and eventual shearing of the borehole at this depth. While additional work is ongoing, no evidence of reactivation on multiple slip surfaces has been identified, indicating that the landslide movement was constrained to a single failure surface at the time of the radar monitoring.

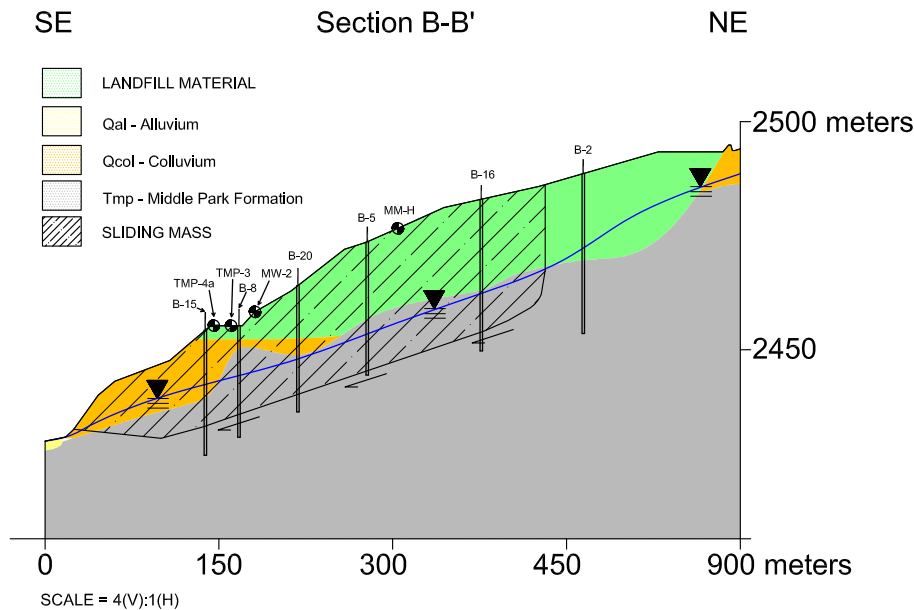


Fig. 3. Interpreted cross section showing boreholes, geologic units, slip plane, and groundwater elevation. Surface movement monuments monitored with GPS are shown, including MM-H, MM-J, MM-O and MM-M.

Landslide movement was first observed in spring 2007 with a displacement rate of approximately 0.01 m/day. The rate of movement has been monitored via traditional survey on a monthly basis since 2007 and on a weekly basis during 2011. The velocities have been calculated using repeated surveys 7–30 days apart and do not resolve diurnal changes in the displacement field. The GPS surveying tracks displacements using real time kinematic GPS, relying on a stable base station off the landslide to resolve monument movements on the landslide. These velocities are calculated in three-dimensions (3D), but are tracked in this paper as horizontal displacements, as the contribution from the vertical settlement is negligible due to shallow dipping (5°) translational failure. A total of 66 survey monuments have been installed during the initial investigation; 21 of those monuments were destroyed due to landslide or construction activity.

Landslide movement varies seasonally, with peak movements coincident with groundwater table (GWT) rise from snowmelt. Landslide movement reached peak velocities of 0.015–0.20 m/day in spring 2011. Landslide velocity has varied seasonally each year in correlation with seasonal variation in the GWT. Fig. 4 presents the range of survey-derived displacement velocities (m/day) and the change in GWT (m) of select monuments for a 12 month cycle. These measurements indicate a generally uniform flow field of displacements, indicating a primarily translational failure, with a ratio of depth of rupture to length of rupture (D_r/L_r) in 0.1, typical of translational failures (Skempton and Hutchinson, 1969). Mapping of slide boundaries have been conducted by field identification of surface shear zone indicators on translational boundaries, tension cracks and scarp features at landslide crown, and heaved or overriding soils at the landslide toe.

3. Methodology

3.1. Line of sight measurements and radar displacement measurement

Radar interferometry is conducted by comparing the phase and amplitude components of two or more radar images to detect and monitor small changes (mm-scale) in the Earth's surface that are undetectable by typical optical imaging (Massonnet and Rabaute, 1993). Analysis of the phase difference between two or more images provides a measurement of the change of distance to the ground surface between the two images, and the phase shift between image measurements reflects changes in the distance between the sensor and the ground surface, i.e., displacement in the LOS direction. The relationship between phase difference and displacement is given by:

$$\delta_{\text{line of sight}} = \frac{-\lambda \delta \phi}{4\pi} \quad (1)$$

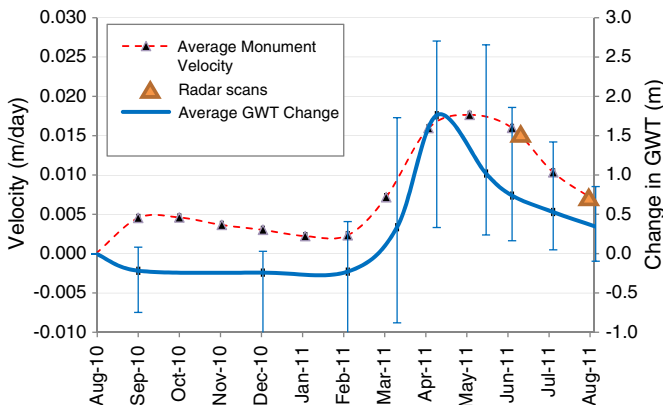


Fig. 4. Average GWT change and average survey monument displacement rate. Radar scans were deployed in June and August of 2011. Range of values shown in error bars.

The sensitivity of interferometric radar to displacement is therefore determined by the wavelength λ of the radar since the phase change ϕ can only be measured between a 4π change given 2-way travel of the radar pulse. As displacement measurements are made in LOS, positioning of radar site in terrestrial platforms is a critical part of planning an effective monitoring program. In the case of the Granby landslide, information about landslide movement and direction was available from existing geotechnical investigation, allowing LOS sensitivity to be anticipated before radar imagery was collected. Given the mobility of the GBIR platform though, monitoring could also be conducted in a reconnaissance mode, deployed without a priori information to constrain movements from multiple scan positions at the cost of temporal continuity.

3.2. Radar system configuration

The radar was deployed across a valley from the Granby landslide with a field of view looking due east (Figure 2). The LOS displacement from this angle is oblique to the landslide's motion by about 45° at the center of the landslide block with obliquity angles varying through the radar image due to rotational scanning action of the GPRI platform. This obliquity is compensated for in post-processing. The GPRI system was equipped with a Ku band antenna capable of resolving mm movement using a wavelength of 1.76 cm (Werner et al., 2008). Further system configuration and instrumental parameters are summarized in Table 2. The GPRI sensor has a range resolution of 0.75 m and a range dependent azimuth resolution of about 7 m at 1 km. The range of the scan position to the landslide varies between 350 m and 800 m or an azimuth resolution that varies from 2.5 m to 5.6 m. Two time-lapse radar surveys were conducted in June and August 2011, respectively, from the same monumented position. An 80° field of view with a 2.5 km range limit was selected to encompass the full view of the mapped landslide boundaries (Figure 2) established from previous mapping. Individual scan times were approximately 15 s and repeated with a minimum interval of 7.5 minute to maximum 15 minute interval between scans. Antenna incidence angle was set at horizontal to maximize the detection of horizontal (translational) displacement, the primary motion in this landslide.

Beyond physical configuration, processing of the acquired radar imagery requires a number of steps to properly conduct the differential interferometry and calculate LOS displacements. The specific combination and parameterization of these separate steps are accomplished with a combination GAMMA provided software, geospatial calculations, and file processing, resulting in a customized workflow that is suited for landslide monitoring with objectives in temporal continuity.

3.3. Imagery processing and interferogram generation

All images were co-registered with the first scene in the time series, and offsets were calculated using cross-correlation matching of small sub-image chips distributed throughout the radar images. Offsets in radar images were corrected with 1st order polynomial resampling to

Table 2
Radar system configuration.

Type	Real aperture FMCW
Manufacturer	Gamma RS
Antenna length	2 m
Frequency	17.2 GHz (Ku band)
Wavelength	1.76 cm
Range resolution	75 cm
Azimuth resolution	Range dependent: 3.5 m @ 500 m, 7 m@1 km
Displacement sensitivity	<1 mm LOS Werner et al. (2008)
Temporal resolution	7–15 min
System deployment time	15 min

ensure proper coregistration of the collected SLC image stack. Interferograms were created from a network of temporally adjacent scene acquisitions within the June and August surveys, respectively. For each scan, offset-corrected, single look complexes (SLCs) or scenes were interfered in the phase spectrum of the imagery to generate interferograms. A temporal network of interferograms was created by interfering coregistered SLCs from 3 scenes before and 3 scenes after each 15 minute SLC acquisition. This approach is functionally similar to an SBAS-type algorithm (Berardino et al., 2002), though spatial baseline in our case is zero. While interferometry could theoretically be conducted for every SLC pair, temporally adjacent SLCs provide the least decorrelation. Some noise reduction is useful in filtering scene-to-scene atmospheric noise. For the interferometry network for a single scene, a small temporal baseline limit of <60 min establishes a network of 6 interferograms. When this set is stacked through averaging, the resulting image provides a sufficient reduction in interferogram noise while preserving efficient processing. The analysis approach used during both surveys is illustrated in Fig. 5. Interferograms spanning the two radar surveys were not created due to the large time span and large movement and phase decorrelation of the landslides between these two time periods.

3.4. Phase unwrapping and displacement inversion

Individual interferograms were filtered using a slope-adaptive filter to improve unwrapping to displacements. Phase unwrapping was accomplished using a minimum-cost flow algorithm (Costantini, 1998; Chen and Zebker, 2000). After phase unwrapping, some interferograms contained a linear phase ramp that most likely represents a tropospheric path delay rather than a true offset. Such atmospheric effects are likely due to variable humidity levels during a scanning survey, and these correlate well with the humidity log for the August survey. We removed the atmospheric phase by modeling a linear phase ramp and subtracting it from the interferogram after Zebker et al. (1997).

A time series was interpolated using the individual interferogram in an over-determined, linearized least-squares inversion (e.g. Schmidt and Bürgmann, 2003). Displacement inversion requires consistently high coherence imagery. The aim of this step was to produce a time series of interferometric phase for each image acquisition time. Using each radar image in multiple interferograms reduced the noise in the

resulting time series. The resulting time series of interferometric phase was then converted to LOS displacements based on the radar wavelength (0.0176 m) and the viewing geometry. Sources of error in the interferograms include system noise which can be smoothed and averaged out through stacking and unwrapping errors due to improper phase ambiguity resolution, which can be recognized easily by jumps in the displacement by half the wavelength.

GPS survey measurements show a uniform velocity field that can be used to correct LOS obliquity using the geometry of the radar scan and topographic aspect calculated from the radar derived digital elevation model (DEM). Also, the imagery was collected in a horizontal LOS, making the interferometry sensitive only to horizontal displacement and insensitive to changes in elevation.

Displacement maps were geocoded using a high-resolution DEM derived from airborne LiDAR collected through the USGS CLICK as part of the National Elevation Dataset (Stoker et al., 2006; Gesch et al., 2007). The radar results were then integrated into a geographical information system (GIS) that allowed for cross referencing of the image to known features on the landslide slope and comparison to previous mapping efforts including independently mapped landslide block boundaries and surveying monuments. Low angle shadowing of the radar field of view allowed for verification geocoding of the radar imagery with topographic shadowing and feature matching.

4. Results

4.1. Imagery and interferogram quality

The radar surveys successfully imaged the majority of the landslide from this field of view, with moderate topographic shadowing. Some strong-returning signals associated with structures on the landslide are present in the imagery near the landslide, such as the fence lines near the toe of the landslide and running longitudinally in the imagery near the center of the scene (Figure 6). Although the imagery was generated entirely from a single scan position, a functional zero baseline, some offsets did exist and were corrected within the imagery. Overall, images generated from scanning were of sufficient quality to generate interferograms that could be used to derive displacements for 11.5 non-continuous hours in the June survey and 36 continuous

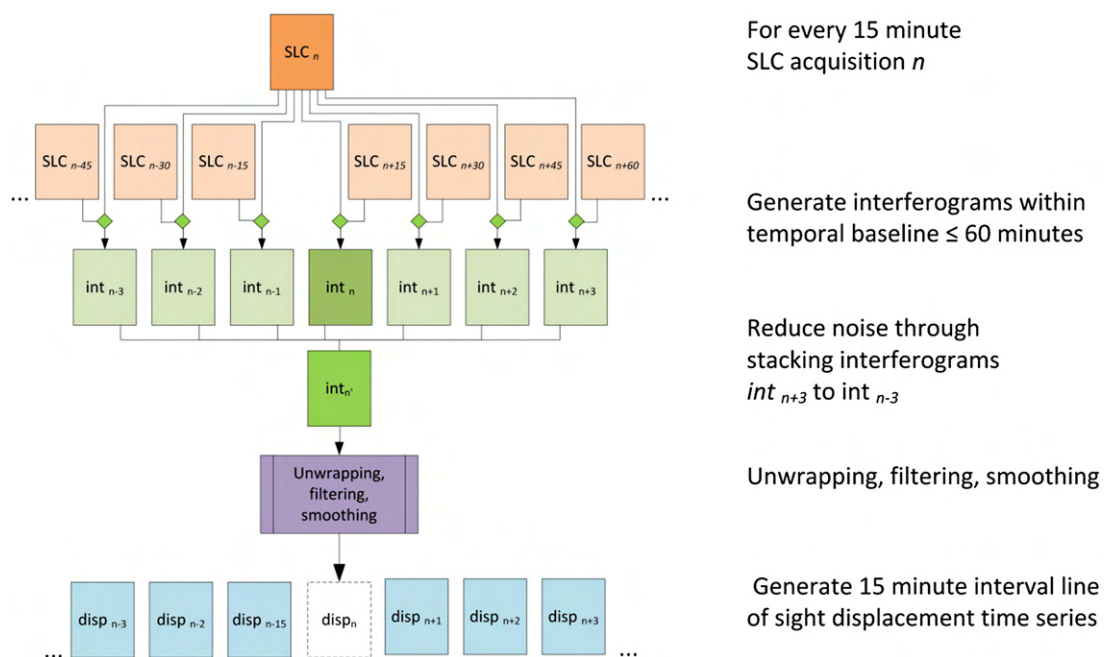


Fig. 5. Interferogram generation and time series displacement dataflow.

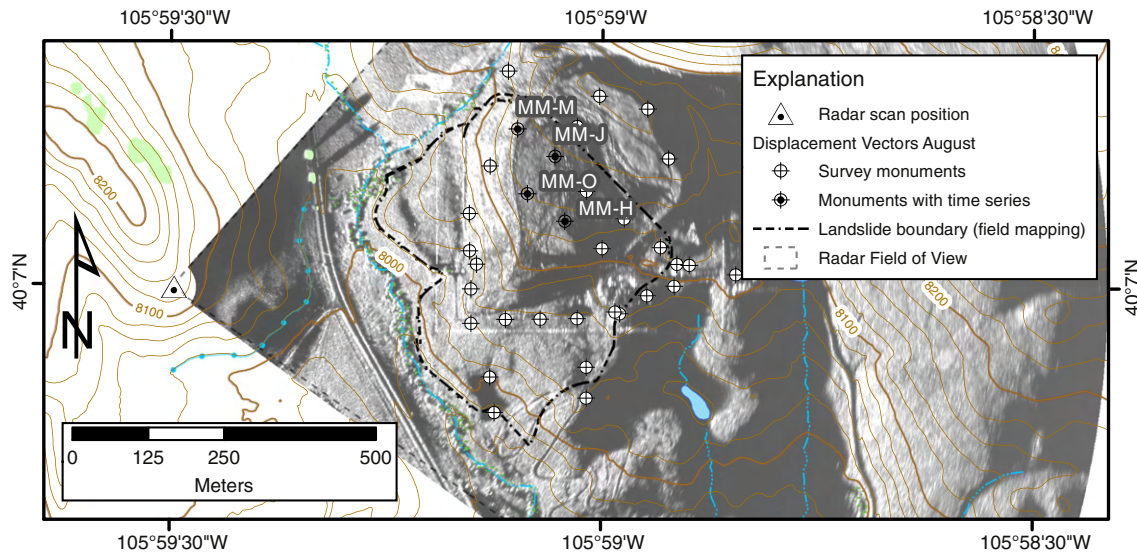


Fig. 6. Typical radar imagery showing amplitude component collected during the June 2011 radar survey. Amplitude component image is scaled from high power (white) to low power (dark gray).

hours in the August 2011 survey. In June, displacements were calculated between 7:30 to 13:00 on June 10, 2011 and between 4:00 am and 9:00 am on June 11th, 2011. Low coherence imagery prevented interferometry for a gap of 5 h in the collected imagery in the June 2011 survey. While other sources of scene-to-scene decorrelation may be present, construction activities of re-grading and material additions likely contributed to most decorrelation of the imagery. On August 14, 2011, coherent imagery was used to create displacement maps from the hours of 20:00 to approximately 10:00 on August 16th. A typical amplitude image of a radar scan is shown in Fig. 6, illustrating topographic shadowing and the strength of signal return in various parts of the scene. Pixel size footprints on the surface vary with range; but are generally about 2 m (azimuth) by 0.75 m (range) at the toe and about 4 m (azimuth) by 0.75 m (range) near the crown.

4.2. Radar measured displacements and survey comparison

Importantly, the GPS surveying was conducted independently as part of ongoing stabilization activities. GBIR monitoring was not coordinated with ongoing construction activities resulting in staggering of dates for GPS survey and radar monitoring. This results in limitations in the temporal coincidence of the GPS-radar comparison. This compounds the disparity in measurement sensitivity and temporal sampling differences between the RTK based GPS measurements and radar interferometry. Therefore the goal of the comparison is to verify the average velocities of the radar monitoring against GPS based surveying. This comparison allows for confirmation of the general accuracy of the technique, as well as facilitates a discussion of strengths and limitations of GBIR being applied to landslide investigations with typically available methods.

After unwrapping and filtering, LOS radar displacements were observed in both surveys. This discussion focuses on analysis of LOS displacements due to the goal of evaluating the performance of GBIR against more traditional methods which are measured in actual displacements. Quantitative verification of GBIR is best suited to a discussion of LOS observations as GBIR is necessarily conducted with the sensors reference frame. Fig. 7 presents processed displacements over both surveys at 1 and at 5 h. Faint displacements are apparent after 1 h and clearly identifiable in June, but August monitoring does not reveal the landslide bounds till further into monitoring due to the decelerated rate.

Fig. 8 presents stacked displacements in terms of daily displacement rate from both surveys. Orthorectified radar imagery clearly maps the

landslide boundaries, with contrasts between zones of horizontal displacement and stable ground. Maximum LOS displacements of 0.018 m and 0.09 m were observed during the 11.5 h June and 36 h August surveys, respectively. These images resolve clear features of the landslide, including a translational shear boundary on the northern landslide boundary, horizontal displacement at the toe, and even a clear boundary between slide block and crown at the upper part of the landslide block, especially apparent in June imagery. The southern boundary is diffuse, indicating more of a shear zone than a shear plane, though this zone is somewhat obscured by terrain shadowing. Also, this zone may be exhibiting displacements in the vertical that are only revealed by the change in LOS horizontal component by the radar images, implying the need for multiple scan positions in the future.

Comparisons with GPS were conducted by selecting the pixel on unwrapped interferogram where the monument was located. Four monuments, MM-H, MM-J, MM-M, and MM-O, were selected to compare daily average velocities from the period of radar monitoring to the GPS derived velocities in both June and August are included in Table 3. These monuments were visible from the radar scan position and located on the central part of the landslide block. A full table of radar and GPS derived velocities is included in Table 4 (supplemental). Other monuments were selected for comparison when visible by the radar and are included in the bulk comparison, discussed below.

Displacements generally increased linearly with time, with some observable scatter. Fig. 9 presents a comparison of radar derived displacement rate versus the LOS component of the traditional survey derived displacement rate. Mean daily displacement rates were estimated from the linear trend lines through the time series displacement data. Despite the difference in timing of GPS surveys and radar monitoring, the average radar and survey derived velocities are well correlated. Scatter and offset in these data are due to differences in survey period, local variation due to model smoothing after phase unwrapping, and topographic shadowing that under-sample the terrain in the radar survey. General agreement between radar and GPS-survey derived velocities verify the overall approach of this platform and workflow to monitor displacement rates on a slow moving landslide. The comparison shows general agreement and clearly indicates the higher displacement rate of the landslide in June and the lower displacement rate in August. The deviation from unity in the August survey indicates a faster displacement rate measured by the GPS survey which occurred before the radar survey. The GPS survey averages displacement rates over a 2 week period during the overall seasonal deceleration of the landslide

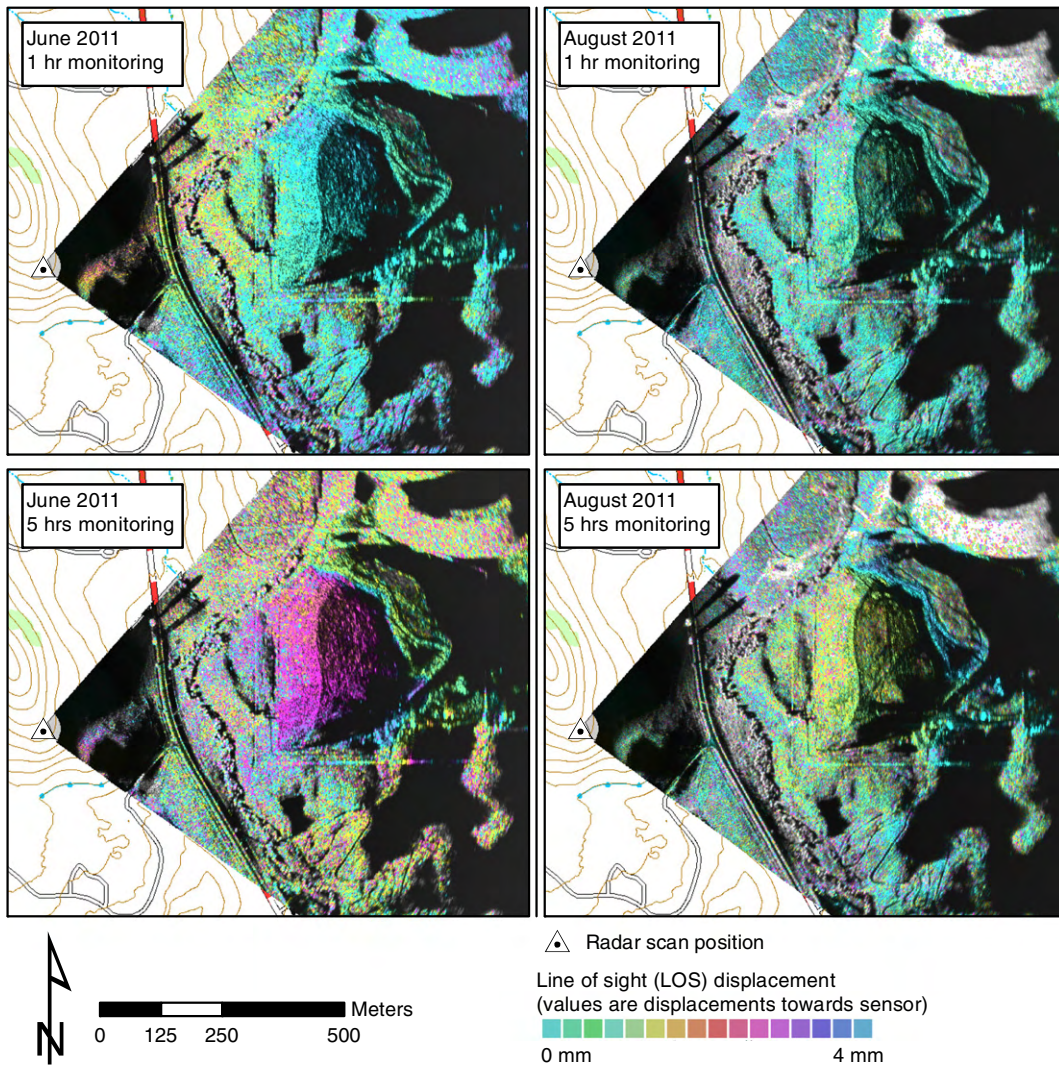


Fig. 7. Typical interferometry from June and August 2011 surveys. Note the increase displacement after 5 h in June 2011 survey compared to the slower displacement rate in August 2011.

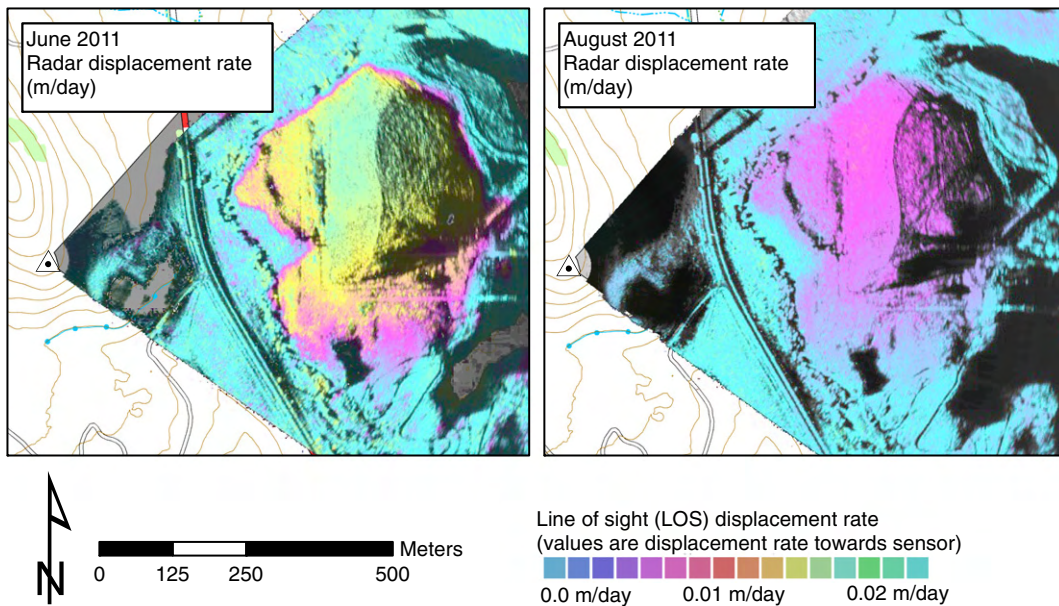


Fig. 8. Average total displacement rate from stacked, unwrapped displacements. Note clearly identifiable displacement boundaries, at translational shear zones, block separation at crown, and overriding toe.

Table 3
Radar and selected GPS derived line of sight displacement rate estimate comparison.

Monument	Radar derived mean displacement rate (LOS)	GPS survey derived mean displacement rate (LOS)
June 2011	10/6/11 over 12 h	7/6/11–14/6/11
MM-H	0.0152 m/day	0.0152 m/day
MM-J	0.0173 m/day	0.0161 m/day
MM-M	0.0177 m/day	0.0164 m/day
MM-O	0.0173 m/day	0.0131 m/day
August 2011	14/8/11–15/8/11 over 36 h	2/8/11–14/8/11
MM-H	0.0030 m/day	0.0059 m/day
MM-J	0.0035 m/day	0.0074 m/day
MM-M	0.0037 m/day	0.0079 m/day
MM-O	0.0035 m/day	0.0087 m/day

and so are expected to measure faster rates of displacement than the 36 hour radar survey. The standard error of the mean of the time-series interpolation was 0.0035 m for the June 2011 survey and 0.004 m for the August 2011 survey, established statistically through processing of the interferograms, both smaller than the apparent limit of detection for both surveys. This error represents the statistical error of the modeled inversion of LOS displacement unwrapping for the entire time series. This error is therefore specific to the spatial and temporal quality of the imagery for both surveys. Survey measurement error in the August case begins to show the limitation of GPS error for small displacements. Although the RTK method is repeatable at less than 1 cm displacements, positional error may be contributing to the offset of GPS displacement rates in Fig. 9.

Finally, time series displacements of single image locations were created for the selected monuments MM-H, MM-J, MM-M and MM-O, which had continuous uninterrupted imagery and consistently high coherence resulting in a finely resolved, tightly constrained measure of displacement at these locations (Figure 10). Though the displacements are generally consistent with the rates observed through GPS, there are nonlinear temporal changes in velocity observed in the August

survey. These changes in velocity are slight but nonetheless represent dynamic displacement conditions that vary on different locations across the slide. This work shows that GBIR capable of investigating movements on these scales, but longer deployments are necessary for investigating and verifying diurnal fluctuations of velocity. Also, no other instrumentation on the landslide was collecting measurements at the temporal density of the radar measurements (7–15 minute intervals) meaning that no confirmatory data can be used to verify the observed fluctuations at this fine of a timescale. Further investigation with high density measurements must be deployed to confirm the variation in displacement rate as well as longer radar occupations to confirm the observed behavior over multiple days.

4.3. Horizontal displacement modeling

Correction of radar measurements to LOS displacement requires a global correction to the displacements or simultaneous capture from multiple instruments to correct obliquity of scan angle compared to horizontal displacement direction. Since the GBIR system is a rotational scanner, the LOS obliquity varies azimuthally across the scene. Using an average movement direction from previous surveys monument displacements, a final displacement was transformed from LOS to horizontal displacement. To complete the displacement modeling, low coherence zones and topographic shadowing were interpolated through to create a continuous field of landslide surface displacement for both the July and August surveys. These interpolations are presented in Fig. 11.

While translational failure appears to be primary mode of failure, actual horizontal displacement measurements indicate at least some differential displacement is occurring across the landslide mass, with fastest displacement rates observed in the northern portion of the landslide near the head. The change in displacement rate changes smoothly across the block. If there were active slip planes or shear zones internal to the block, these features would result in abrupt changes in displacement imagery and would be indicative of kinematic heterogeneity but none are apparent during either survey. Therefore we conclude that

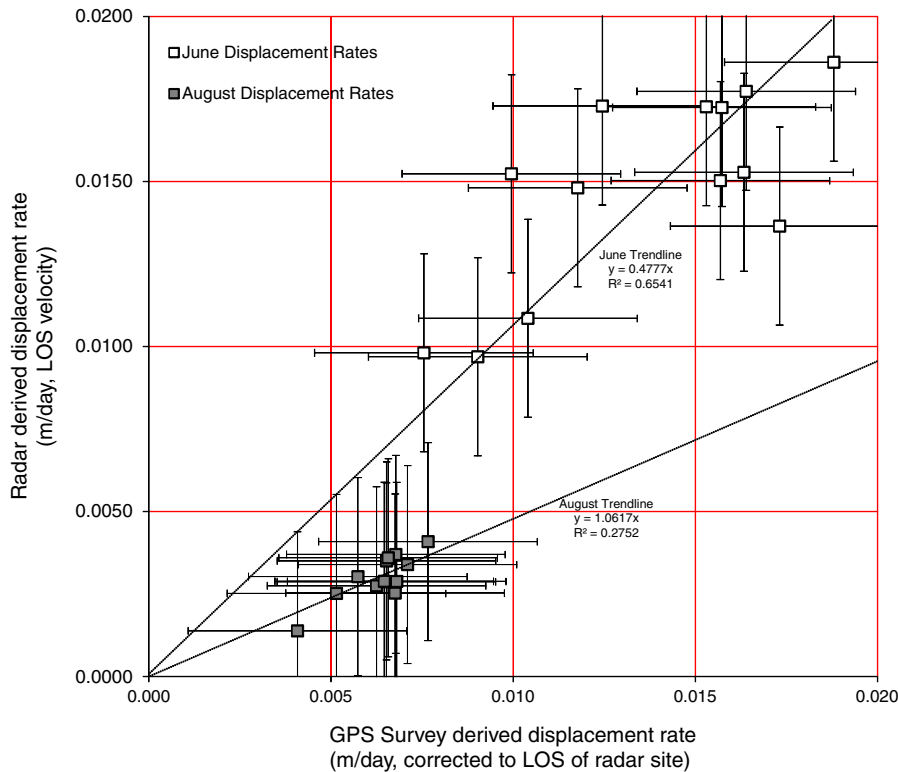


Fig. 9. Comparison of radar and GPS derived displacement rate estimates along LOS of radar system.

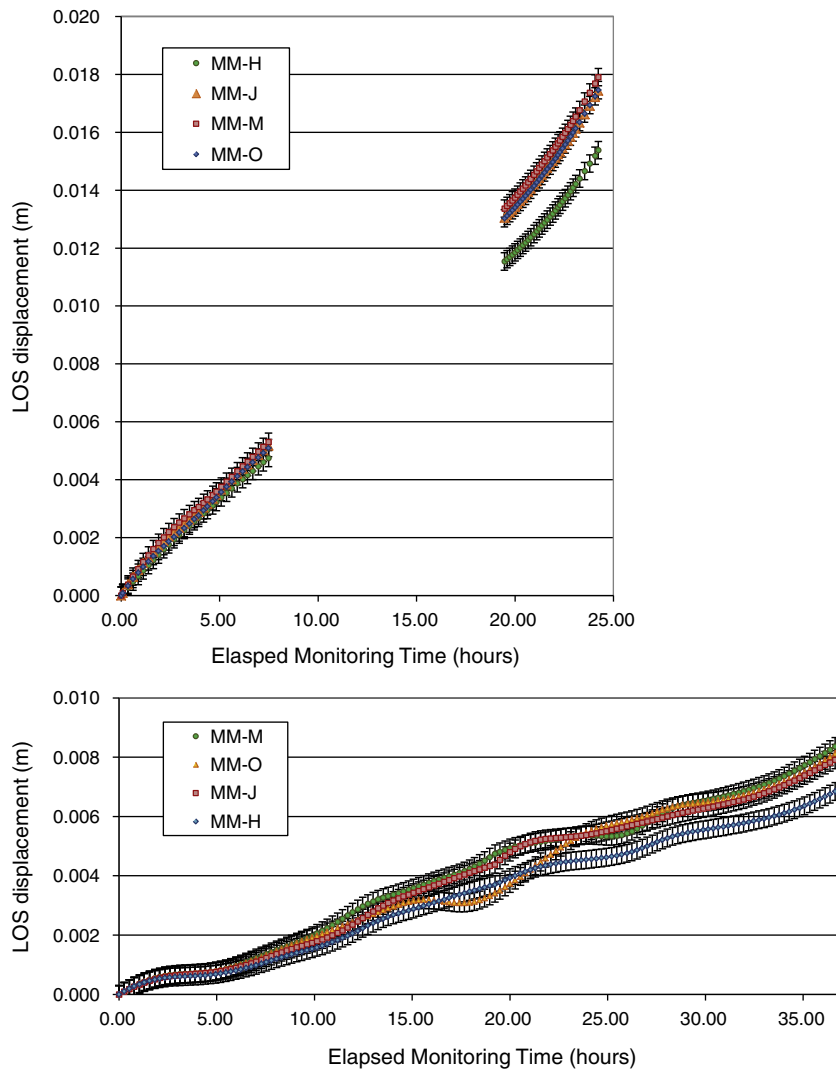


Fig. 10. Time series of radar derived displacements near survey monuments for the June 2011 (top) and August 2011 (bottom) scans. Locations of these monuments are presented on Fig. 6 and velocities are presented in comparison to survey derived displacement rates in Table 3.

no complex failure activity existed at the time of the survey within the main landslide mass, consistent with the accepted conceptual model of a landslide with primarily translational failure. The radar imagery and displacement modeling verifies the conceptual model and allows decisions to be made with less uncertainty. Because of its continuous spatial field and fine scaled temporal granularity, the GBIR monitoring data confirm the lack of kinematic landslide elements that might have existed between GPS survey measurement points.

Due to primary objective of tracking horizontal displacements, this investigation did not resolve vertical displacement measurements. While toe heave and block head settlement are obvious from site investigations, a second survey location will need to be established in the future to monitor displacement in the vertical direction, and generate 3D displacements. For example, a scanning position below the landslide south east of the current position conducted with angled aperture would be expected to detect such displacements, though topographic shadowing from this location would be more prevalent. Alternatively, the ground based investigation could be supplemented by satellite based imaging which is more natively suited to vertical movements.

5. Conclusion and future applications

Landslide displacement using the GPRI platform is capable of detecting and monitoring displacement in mm-scale and useful in

resolving small scale temporal variation in slip rates. By leveraging the zero spatial baseline, this interferometry collection and processing methodology reveals a high level of temporal resolution of the displacements. The measurements of GBIR is compared and in good agreement with measurements made by traditional GPS surveys. The major goal of establishing GBIR with the GAMMA GPRI sensor as a spatially and temporally dense landslide monitoring technique was achieved. Now, as mitigation measures are implemented, this sensor can be relied upon to provide near real-time displacement data, allowing for more integrated use in evaluation of stabilization effectiveness.

The specific combination of the GPRI sensor for this monitoring application is overall well suited to this monitoring application. Some assumptions about actual horizontal displacement must be made due to the rotational nature of the scanner, but our work demonstrates that LOS correction is not problematic in this case. GBIR monitoring may be improved by the application of different sensors or different methods, such as permanent scatterer analysis applied in Barla et al. (2010) and Schulz et al. (2012). Although this landslide investigation was well established at time of GBIR deployment, the GPRI sensor has a number of significant advantages to reconnaissance and early stage evaluation of incipient slope movements. Evidence of nonlinear changes in displacement rates across the slides also indicate the need to deploy for longer multiday occupations with continuous measurement and similarly densely recording geotechnical instrumentation to observe

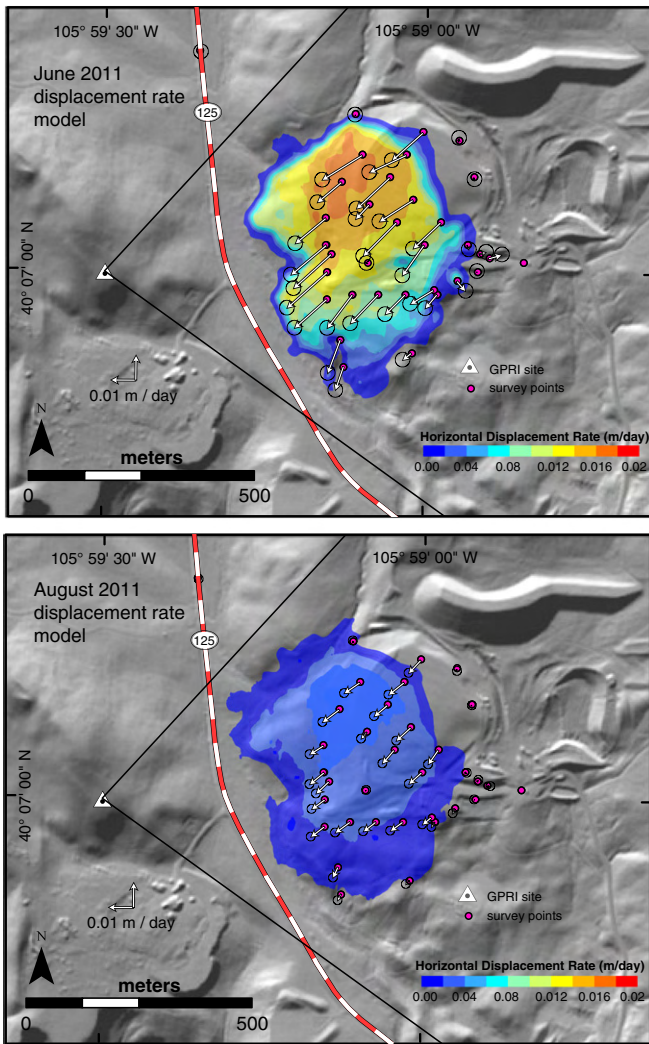


Fig. 11. Radar derived daily horizontal displacement rate models; 24 h of non-continuous monitoring on June 11th, 2011 (top) and 36 h from a survey begun on August 14th 2011 (bottom). Gray background represents stable ground and is displayed as a hillshade of existing topography. Vectors represent scaled monument movement with displacement rates.

diurnal fluctuations or other temporal dynamics of the landslide. Longer multiday deployments of GBIR sensors could significantly aid observation and description of diurnal, nonlinear fluctuations of velocity, such as shear strength changes with atmospheric tides described in Schulz et al. (2009). The presence of these fluctuations justifies high frequency recording of other instrumentation, such as water level transducers and geotechnical instruments. Opportunities for multiple scan locations, with concurrent deployment of two radar sensors are interesting variations of this simplified case, and could be used by investigators to ask questions of landslide kinematics which were impossible to ask before, such as anchor placement effectiveness or evaluation of dewatering pumping on displacement. Also, future analysis and combination with other geodetic tools, such as LiDAR, high rate GPS, and geotechnical data ensure more research on GBIR which will benefit the understanding of this and other landslides.

Supplementary data to this article can be found online at <http://dx.doi.org/10.1016/j.enggeo.2013.07.007>.

Acknowledgments

This work was carried out under multiple NSF grants including MRI equipment award 0923086 and NSF IGERT awards 0801692 as well as collaboration with Grand County authorities and associated consultants. Thanks also to UNAVCO for field assistance and technical consultation.

References

- Barla, G., Antolini, F., Barla, M., Mensi, E., Piovano, G., 2010. Monitoring of the Beauregard landslide (Aosta Valley, Italy) using advanced and conventional techniques. *Eng. Geol.* 116, 218–235.
- Berardino, P., Fornaro, G., Lanari, R., Sansosti, E., 2002. A new algorithm for surface deformation monitoring based on small baseline differential SAR interferograms. *IEEE Trans. Geosci. Remote Sens.* 40, 2375–2383.
- Bossler, J.D., Jensen, J.R., McMaster, R.B., Rizos, C., 2002. *Manual of Geospatial Science and Technology*. Taylor & Francis, London; New York.
- Casagli, N., Catani, F., Del Ventisette, C., Luzi, G., 2010. Monitoring, prediction, and early warning using ground-based radar interferometry. *Landslides* 7, 291–301.
- Cascini, L., Fornaro, G., Peduto, D., 2010. Advanced low-and full-resolution DInSAR map generation for slow-moving landslide analysis at different scales. *Eng. Geol.* 112, 29–42.
- Chen, C.W., Zebker, H.A., 2000. Network approaches to two-dimensional phase unwrapping: intractability and two new algorithms. *JOSA A* 17, 401–414.
- Colesanti, C., Wasowski, J., 2006. Investigating landslides with space-borne Synthetic Aperture Radar (SAR) interferometry. *Eng. Geol.* 88, 173–199.
- Costantini, M., 1998. A novel phase unwrapping method based on network programming. *IEEE Trans. Geosci. Remote Sens.* 36, 813–821.
- Cruden, D.J., Varnes, D.J., 1996. Landslide types and processes. *Landslides: Investigation and Mitigation*. Transportation Research Board Special Report, pp. 36–75.
- Gesch, D., Mauck, J., Hutchinson, J., Carswell Jr., W.J., 2007. *The National Map—Elevation: U.S. Geological Survey Fact Sheet 106-02 (USGS Fact Sheet)*. United States Geological Survey, USGS Eastern Region PSC 4.
- Grand County Government, Gagnon, T., 2011. *Grand County Landfill Landslide Stabilization Request for Proposal for Design Services*. Grand County.
- Hilley, G.E., Bürgmann, R., Ferretti, A., Novali, F., Rocca, F., 2004. Dynamics of slow-moving landslides from permanent scatterer analysis. *Science* 304, 1952–1955.
- Lee, I.-S., Ge, L., 2006. The performance of RTK-GPS for surveying under challenging environmental conditions. *Earth Planet. Space* 58, 515–522.
- Leva, D., Nico, G., Tarchi, D., Fortuny-Guasch, J., Sieber, A.J., 2003. Temporal analysis of a landslide by means of a ground-based SAR interferometer. *IEEE Trans. Geosci. Remote Sens.* 41, 745–752.
- Massonet, D., Rabaute, T., 1993. Radar interferometry: limits and potential. *IEEE Trans. Geosci. Remote Sens.* 31, 455–464.
- Noferini, L., Pieraccini, M., Mecatti, D., Macaluso, G., Atzeni, C., Mantovani, M., Marcato, G., Pasuto, A., Silvano, S., Tagliavini, F., 2007. Using GB-SAR technique to monitor slow moving landslide. *Eng. Geol.* 95, 88–98.
- Rizos, C., 1999. *GPS enhancements. Notes on Basics GPS Positioning and Geodetic Concepts*. School of Surveying and Spatial Information, University of New South Wales.
- Schmidt, D.A., Bürgmann, R., 2003. Time-dependent land uplift and subsidence in the Santa Clara valley, California, from a large interferometric synthetic aperture radar data set. *J. Geophys. Res.* 108, 2416.
- Schroder, D., 1995. *Geologic Map of the Granby Quadrangle, Grand County, Colorado (Geologic Quadrangle Map No. GQ-1763)*.
- Schulz, W.H., Kean, J.W., Wang, G., 2009. Landslide movement in southwest Colorado triggered by atmospheric tides. *Nat. Geosci.* 2, 863–866.
- Schulz, W.H., Coe, J.A., Shurtleff, B.L., Panosky, J., Farina, P., Ricci, P.P., Barsacchi, G., 2012. Kinematics of the Slumgullion landslide revealed by ground-based InSAR surveys. In: Eberhardt, E., Froese, C., Turner, K., Leroueil, S. (Eds.), *Landslides and Engineered Slopes, 2 Volume Set + CDROM*, Protecting Society Through Improved Understanding. CRC Press, Taylor & Francis, London, p. 2050.
- Skempton, A.W., Hutchinson, J.N., 1969. Stability of natural slopes and embankment foundations. In: *Proceedings of the Seventh International Conference on Soil Mechanics and Foundation Engineering*. Sociedad Mexicana de Mecana de Suelos, Mexico City. State of the Art Volume, pp. 291–340.
- Stoker, J.M., Greenlee, S.K., Gesch, D.B., Menig, J.C., 2006. CLICK: the new USGS center for lidar information coordination and knowledge. *Photogramm. Eng. Remote Sens.* 72, 613–616.
- Strozzi, T., Farina, P., Corsini, A., Ambrosi, C., Thüring, M., Zilger, J., Wiesmann, A., Wegmüller, U., Werner, C., 2005. Survey and monitoring of landslide displacements by means of L-band satellite SAR interferometry. *Landslides* 2, 193–201.
- Tarchi, D., Casagli, N., Fanti, R., Leva, D.D., Luzi, G., Pasuto, A., Pieraccini, M., Silvano, S., 2003. Landslide monitoring by using ground-based SAR interferometry: an example of application to the Tessina landslide in Italy. *Eng. Geol.* 68, 15–30.
- Werner, C., Strozzi, T., Wiesmann, A., Wegmüller, U., 2008. Gamma's portable radar interferometer. In: *13th FIG Symposium on Deformation Measurements Ad Analysis*. LNEC, Lisbon, p. 16 (May).
- Zebker, H.A., Rosen, P.A., Hensley, S., 1997. Atmospheric effects in interferometric synthetic aperture radar surface deformation and topographic maps. *J. Geophys. Res.* 102, 7547–7563.